論文 / 著書情報
Article / Book Information

Title	A Wideband 16 × 16-Element Corporate-Feed Hollow-Waveguide Slot Array Antenna in the 60-GHz Band
Authors	Takashi Tomura, Jiro Hirokawa, Takuichi Hirano, Makoto Ando
Citation	IEICE Transactions on Communications, Vol. E97-B, No. 4, pp. 798-806
Pub. date	2014, 4
Copyright	Copyright (c) 2014 Institute of Electronics, Information and Communication Engineers.

IEICE TRANS. COMMUN., VOL.E97–B, NO.4 APRIL 2014

PAPER

A Wideband 16 × 16-Element Corporate-Feed Hollow-Waveguide Slot Array Antenna in the 60-GHz Band

Takashi TOMURA[†a)], ***Student Member***, **Jiro HIROKAWA**[†], ***Senior Member***,
Takuichi HIRANO[††], ***Member***, ***and*** **Makoto ANDO**[†], ***Fellow***

SUMMARY A 16 × 16-element corporate-feed waveguide slot array antenna in the 60-GHz band is designed to achieve broadband reflection and high antenna efficiency. The sub-arrays consisting of 2×2-elements are designed to improve the reflection bandwidth by implementing lower Q and triple resonance. The designed antenna is fabricated by diffusion bonding of thin copper plates. A wide reflection bandwidth with VSWR less than 2.0 is obtained over 21.5%, 13.2 GHz (54.7–67.8 GHz). The measured gain is 32.6 dBi and the corresponding antenna efficiency is 76.5%. The broad bandwidth of more than 31.5-dBi gain is realized over 19.2%, 11.9 GHz (56.1–68.0 GHz). The gain in bandwidth covers the whole of the license-free 60-GHz band (57–66 GHz).

key words: *corporate feed, millimeter-wave band, waveguide slot array, wideband*

1. Introduction

Millimeter-wave and sub-millimeter wave bands are promising candidates for high speed wireless communication of more than several Gbps. Wireless communication systems using 9-GHz (14.6%) bandwidth in the 60-GHz band (57–66 GHz) [1] and 17-GHz (13.6%) bandwidth in the 120-GHz band [2] have been proposed. For fixed wireless links, a high gain antenna with wideband characteristics of gain and reflection is required to realize the high speed communication needed. Hollow-waveguide slot array antennas have been widely used for fixed wireless communication and radar systems in the microwave and millimeter-wave bands [3]. They can achieve a high gain, above 30 dBi, with high antenna efficiency even in the millimeter-wave band because of the low transmission loss. Further, difficulties in mass production, one of the biggest drawbacks of hollow-waveguide slot arrays, are avoided by the simple composition and fabrication methods. A single layer slotted waveguide array antenna [4], [5], which consists of only two parts fixed by screws, has been adopted for a fixed wireless access system [5]. Horn arrays [6] and a multi-layer waveguide slot array [7] have been fabricated by diffusion bonding of thin etched-plates. This method enables fabrication of multi-layer structures and makes mass production possible.

Manuscript received July 26, 2013.
Manuscript revised November 29, 2013.

[†]The authors are with the Department of Electrical and Electronic Engineering, Tokyo Institute of Technology, Tokyo, 152-8552 Japan.
[††]The author is with the Department of International Development Engineering, Tokyo Institute of Technology, Tokyo, 152-8552 Japan.
a) E-mail: tomura@antenna.ee.titech.ac.jp

DOI: 10.1587/transcom.E97.B.798

However, waveguide slot array antennas generally have narrow bandwidths due to the frequency dependence of the feed structures and the impedance bandwidth of the radiating slots. Feeding methods may be divided into two: series- and corporate-feeds. A series-feed structure is commonly used since it realizes the shortest feeding distance leading to the lowest transmission loss. The disadvantage of the series-feed is a narrow directivity bandwidth because of phase variations, depending on the frequency, the so-called long-line effect. To obtain wider directivity bandwidth, structures composed of corporate-feed and series-feed sub-arrays have been proposed [8]–[10]. However, the directivity bandwidth is restricted by the number of elements in the series-fed sub-array.

Corporate-feed enables in-phase excitation independent of frequency or number of elements, making a wide directivity bandwidth possible even for a large number of elements. Wideband corporate-feed waveguide slot arrays with more than 30-dBi gain have been reported [11], [12]. Here the sub-arrays consist of a cavity-backed slot array which is excited in phase independent of the frequency. In [11], a 16 × 16-element antenna composed of 2 × 8-element sub-arrays achieved a 33.1-dBi gain, 85.0% antenna efficiency, and a 12% impedance bandwidth of VSWR below 2.0 in the 12-GHz band. In [12], a 16 × 16-element antenna composed of 2 × 2-element sub-arrays achieved a 33.0-dBi gain, 83.6% antenna efficiency, and 11% one-dB down gain bandwidth in the 60-GHz band. The gain in bandwidth of both these two antennas is limited by the impedance bandwidth of the sub-arrays. However, improvement of the impedance bandwidth of the sub-arrays has not been sufficiently investigated.

Several attempts have been made to improve the impedance bandwidth of the radiating elements such as slots and patches. In order to reduce Q, a wide slot has been adopted [13] and the dielectric constant and thickness of the microstrip antenna are properly determined [14]. Parasitic elements have been placed beside a patch antenna to realize double resonance characteristics [15], [16]. However, these papers do not consider an extension including a large number of elements. Further, the number of optimized parameters are limited to four [12] because of the computation time using commercial software.

The novelty in the present paper lies in the way (methodology) the bandwidth for the sub-array consisting of 2 × 2-elements is improved. In this paper, based on [12],

a sub-array consisting of 2 × 2-elements is designed with careful attention to improve the impedance and gain bandwidth of arrays wider than the 60-GHz band (14.6% bandwidth). A rapid method of analysis of the sub-array is established and enables optimizing 11 parameters. Further, by introducing the triple resonance, the bandwidth of the sub-array is improved as much as 20.4%. For the analysis of the sub-array, the method of moments (MoM) with numerical eigenmode expansion [17] is used. In the design, wider radiating slots are adopted to achieve lower Q so that triple resonance reflection characteristics is introduced. A 16×16-element waveguide slot array composed of the designed sub-arrays is fabricated by diffusion bonding of laminated-thin plates. The measured results are presented and discussed together with the simulated results.

2. Configuration and Operation Mechanism

The 16 × 16-element plate-laminated-waveguide slot array is shown in Fig. 1. The design frequency is 61.5 GHz. The array is composed of two parts: the feeding part in the lower layer and the radiating part in the upper layer. The antenna is fed through the feeding aperture from its back. The feeding circuit is a corporate feed and a combination of H-plane T-junctions. The coupling aperture is located at each end of the feeding circuit to enable feed of the radiating part in phase and with equal amplitude. The radiating part is composed of the 2 × 2-element sub-arrays shown in Fig. 2. Four radiating slots are placed on a cavity with a 4.2-mm (0.86 λ_0) constant spacing in the x and y directions and excited in phase with equal amplitude.

3. Analysis Method of 2 × 2-Element Sub-Array

The aim of this study is to realize broadband reflection suppression and a high gain over more than 14.6% of the bandwidth (the 60-GHz bandwidth). The feeding circuit is the same as the one presented in [12] and it has realized 19.6% of the bandwidth for VSWR < 1.5, which is a prerequisite to realize the wideband array antenna. However, the bandwidth of the sub-array for VSWR < 1.5 is 9.1%, and only the 2 × 2-element sub-array has to be redesigned to improve on this figure.

The model for the analysis of the 2 × 2-element sub-array is shown in Fig. 2. Two pairs of periodic boundary walls are assumed to include mutual coupling effects among an infinite two-dimensional array of sub-arrays. The design frequency band is from 53.0 to 70.0 GHz with the center frequency 61.5 GHz. The frequency characteristics of reflection are calculated by MoM with numerical eigenmode expansions [17]. The method shortens the analysis time greatly compared to the commercial general purpose simulation software HFSS, based on the finite element method (FEM).

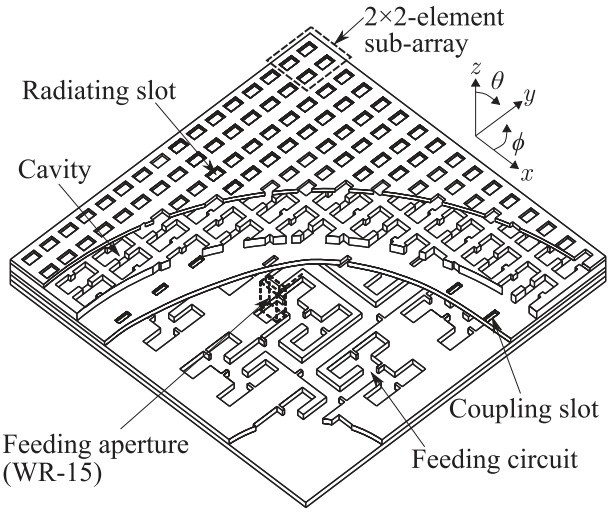

Fig. 1 Configuration of the 16 × 16-element array.

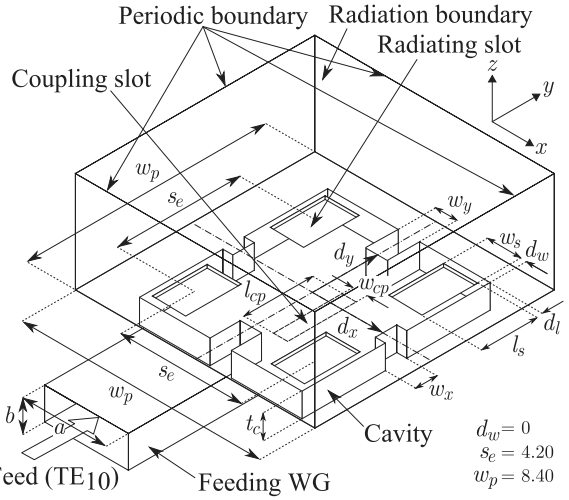

Fig. 2 Model for the analysis of the 2 × 2-element sub-array.

3.1 Method of the Analysis

The model is analyzed by MoM, which solves the tangential component of the electric field on each slot surface, and is used to solve simultaneous integral equations derived from the electromagnetic boundary conditions using the dyadic Green's function. The fields on the slots are expanded by entire-domain vector basis functions. The analysis is conducted in the following three steps.

Step 1) Based on the field equivalent theorem, the bottom and the top surfaces of the coupling and the radiating slots, are replaced by perfect electric conductors (PEC) with equivalent magnetic currents $\mathbf{M}_i$, $i = 1, \ldots, 4$. The field distributions of the four radiating slots are assumed to be equal because of the symmetric structure of the cavity shape. The model is divided into five regions; the feeding waveguide, the coupling slot, the cavity, the radiating slot, and the external region.

Step 2) The equivalent currents $\mathbf{M}_i$ are expanded by vector entire-domain basis functions $\mathbf{m}_{u\alpha\beta}$ and $\mathbf{m}_{v\alpha'\beta'}$ as follows.

$$\mathbf{M}_i = \sum_{p=1}^{P_i} V_{ip}\mathbf{m}_{ip} = \sum_{\alpha=1}^{A_i}\sum_{\beta=0}^{B_i} V_{iu\alpha\beta}\mathbf{m}_{u\alpha\beta} + \sum_{\alpha'=0}^{A'_i}\sum_{\beta'=1}^{B'_i} V_{iv\alpha'\beta'}\mathbf{m}_{v\alpha'\beta'}$$
$$\mathbf{m}_{u\alpha\beta} = \sqrt{\frac{\epsilon_{\alpha\beta}}{lw}}\sin\left\{\frac{\alpha\pi}{l}\left(u+\frac{l}{2}\right)\right\}\cos\left\{\frac{\beta\pi}{w}\left(v+\frac{w}{2}\right)\right\}\hat{\mathbf{u}}$$
$$\mathbf{m}_{v\alpha'\beta'} = \sqrt{\frac{\epsilon_{\alpha'\beta'}}{lw}}\cos\left\{\frac{\alpha'\pi}{l}\left(u+\frac{l}{2}\right)\right\}\sin\left\{\frac{\beta'\pi}{w}\left(v+\frac{w}{2}\right)\right\}\hat{\mathbf{v}} \quad (1)$$

where $V_{iu\alpha\beta}$ and $V_{iv\alpha'\beta'}$ are the weights to be solved; u and v are for the local coordinate system whose origin is each slot center. The u- and v-axes represent the directions along the length and the width, respectively. The basis functions $\mathbf{m}_{u\alpha\beta}$ and $\mathbf{m}_{v\alpha'\beta'}$ have components along the length and the width directions, respectively and α, β, α' and β' are the orders. Further, P_i is the total number of basis functions of $\mathbf{M}_i$ and A_i, B_i, A'_i and B'_i are the maximum orders of the basis function; l and w are the length and the width of the slots, the normalized constant $\epsilon_{\alpha\beta}$ is two when either α or β is zero and otherwise four.

Step 3) Simultaneous integral equations are derived by the continuity conditions of the tangential component of the magnetic field on the apertures with the dyadic Green's function for each region. The application of Galerkin's MoM gives a system of linear equations. By solving the system of the linear equations, the weights of the basis functions are obtained. Then, antenna parameters such as a reflection coefficient, radiation patterns, and directivity gain can be calculated.

The Green's function in the cavity region is expanded by numerical eigenmodes computed by the edge-based FEM [18] because the eigenmodes can not be derived in analytical form due to the X-shaped cross section.

3.2 Results of the Analysis

The results of the analysis by the method detailed above are discussed in this section. The parameters of the model are the conventionally designed sub-array [12]. The frequency characteristics of reflection are shown in Fig. 3 with the results calculated by HFSS ver. 10. The number of basis functions is carefully selected for sufficient accuracy in antenna design. For the coupling slot, one length-component basis function ($P_1 = P_2 = 1$) is used. For the radiating slots, four different numbers of basis functions ($P_3 = P_4 = 33$, 43, 57, 420) are used. The maximum orders (A_3, B_3, A'_3, B'_3) of the basis functions are (3, 10, 0, 0), (3, 10, 5, 1), (3, 10, 5, 4), and (10, 20, 20, 10), respectively. The results using 33 or 43 basis function do not agree with the HFSS result. The result using 57 basis functions shows agreement with that using 420 basis functions and the HFSS result. The calculated normalized weighting coefficients of the radiating slots are shown in Fig. 4 for the case with 420 basis functions. The basis functions of $\alpha = 1$ or $\beta' = 1$ are larger than

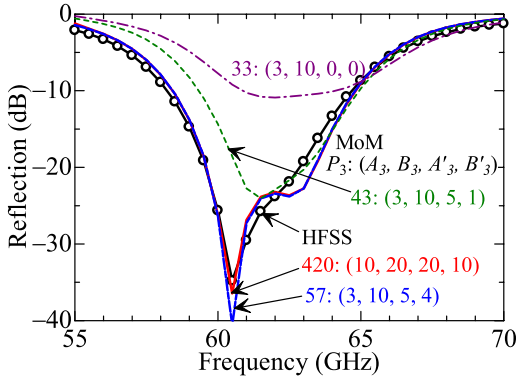

Fig. 3 Reflection coefficients calculated by MoM and HFSS.

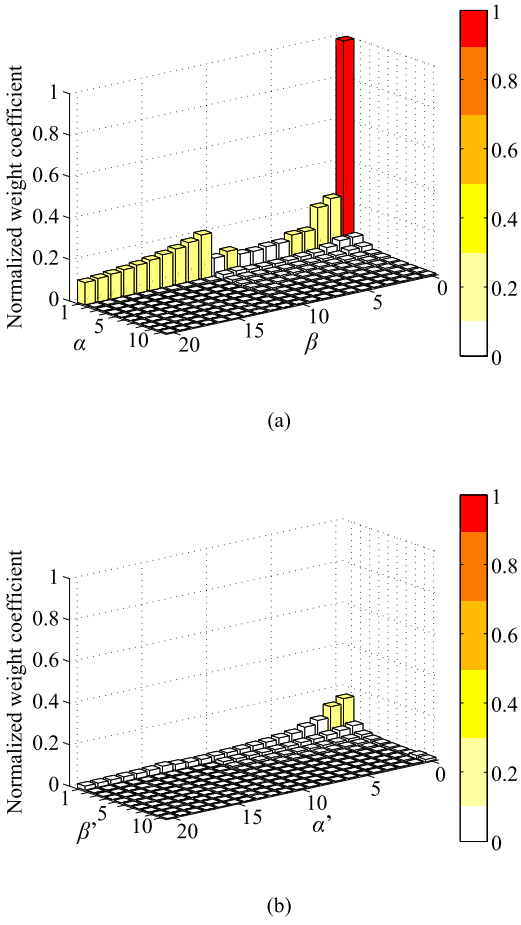

Fig. 4 Normalized weighting coefficients of the radiating slots. (a) u-component. (b) v-component.

the others. These results show that higher order basis functions such as $\beta > 10$ or $\alpha' > 5$ can be disregarded as their calculated weighting coefficients are small and/or the effects on the reflection coefficient is negligible. Even though the weights for $\alpha = 1$ and $\beta > 10$ are large, the reflection coefficients calculated using 57 (excluding $\alpha = 1$ and $\beta > 10$) and 420 (including $\alpha = 1$ and $\beta > 10$) basis functions are the same as is shown in Fig. 3. Although the weighting coefficients of the v-component basis functions are smaller than

those of the u-component ones, they have to be included to ensure sufficient accuracy in an antenna design.

The computation time has been reduced from 20 minutes by HFSS ver. 10 to 9.0 seconds by the method proposed here. The computer used for the calculations has an Intel Core i7 CPU with 2.80 GHz and 8-GB memory. The computations consist of the calculations of the X-shaped cavity eigenmodes and the reflection coefficient at each frequency. The overall time for calculating 31 frequency points is 9.0 seconds, with 4.5 and 3.5 seconds for the eigenmode and reflection coefficient calculations, respectively. It is sufficient to calculate the eigenmodes once as they are independent of the frequency.

4. Design

4.1 Design Procedure for a 2 × 2-Element Sub-Array

The 2 × 2-element sub-array is designed in three steps. By optimizing 11 parameters, the reflection bandwidth of VSWR below 1.5 is improved from 9.2% to 20.4%. The key issues to widen the bandwidth are to reduce the Q of each resonance, increase the number of resonances, and arrange the resonance frequencies properly. Optimizing a large number of parameters by commercial EM software is not practical because of the computation time. The MoM analysis with numerical eigenmode expansion enables the design with 11 parameters. Impedance is designed to be matched so that VSWR is below 1.2 at the design frequency. The resonance frequency is controlled by the coupling and radiating slot length. The initial parameter is the same as the one in [12] and the parameters of each step are listed in Table 1.

Step 1) Wider radiating slots are adopted for lower Q, and the reflection bandwidth is improved from 9.2% to 12.0%. The radiating slot width is increased from 1.75 mm to 2.05 mm in 0.05 mm steps. The impedance is matched by w_y, d_x, and w_x for each radiating slot width w_s. The reflection bandwidth as a function of the slot width is shown in Fig. 5 (Step 1-1) and the maximum bandwidth is 11.0%. In the maximum bandwidth model, the inserted wall width w_y is 0.01 mm for the impedance matching. The inserted wall can be removed because of the symmetrical electromagnetic field distribution in the cavity, and a model without inserted wall is designed. Similarly, the slot width is increased in 0.05 mm steps from 2.05 mm to 2.30 mm and the impedance is matched by d_x, d_l, and w_{cp} for each radiating slot width w_s. The reflection bandwidth increases to 12.0% as shown in Fig. 5 (Step 1-2). The maximum bandwidth is obtained when the slot width is 2.25 mm.

Step 2) The reflection characteristics are changed from double to triple resonance and the bandwidth improves from 12.0% to 18.0%. The locus of the reflection coefficient in a Smith chart is shown in Fig. 6 by the chain line and forms a loop around the origin. This indicates that the reflection characteristics are a double resonance. We found that the outer loop gets smaller by reducing the coupling slot width w_{cp}. The coupling slot width is reduced in 0.05 mm steps from 0.75 mm to 0.20 mm. The impedance is matched by w_s, d_x, and l_{cp} for each coupling slot width. The reflection

Table 1 Dimensions of the designed sub-array in each step.

Step		Initial	1-1	1-2	2-1	2-2	3
Feeding waveguide	a	2.94				3.09	2.88
	b	1.20					
Coupling slot	l_{cp}	2.74			2.48	2.57	2.48
	w_{cp}	1.00		0.75	0.25	0.26	0.25
	t_{cp}	0.30					0.20
Cavity	d_l	0.00		0.85		0.83	0.86
	t_c	1.20					1.00
Walls	d_x	2.26	2.05	2.17	2.19	2.26	2.22
	w_x	0.75	1.30			1.19	0.86
	d_y	1.37		NA			
	w_y	0.75	0.01	NA			
Radiating slot	l_s	2.74	2.87			2.92	3.21
	w_s	1.75	2.05	2.25	2.30	2.20	
	t_s	0.30					0.20

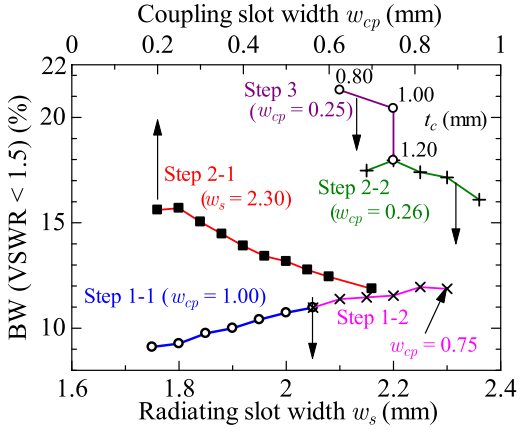

Fig. 5 Reflection bandwidth improvement.

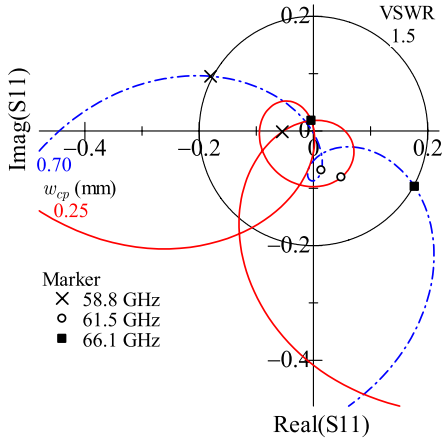

Fig. 6 Reflection characteristics of start and end of step 2-1.

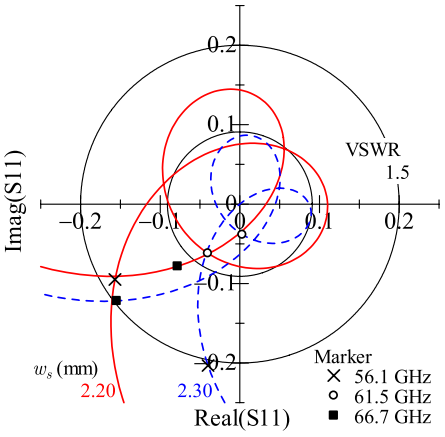

Fig. 7 Reflection characteristics of start and end of step 2-2.

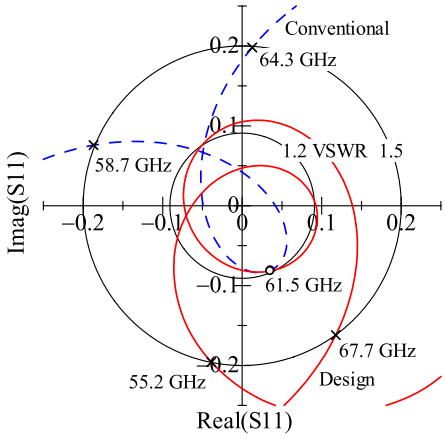

Fig. 8 Reflection characteristics of the conventional and design models.

bandwidth is improved to 15.7% as shown in Fig. 5 (Step 2-1). When w_{cp} is 0.25 mm, the locus of the reflection makes two loops around the origin as shown in Fig. 6. This indicates that the reflection characteristics change to triple resonance. Next, the size of the loops is adjusted by the radiating slot width w_s. The impedance is matched mainly by d_x, w_x, and a and slightly by d_l and w_{cp} for each radiating slot width. As the radiating slot gets narrower, the size of the loops becomes larger as shown in Fig. 7. The reflection bandwidth as a function of the radiating slot width is shown in Fig. 5 (Step 2-2) and an 18.0% wider bandwidth is obtained when w_s is 2.20 mm.

Step 3) The cavity height is designed and the reflection bandwidth improves from 18.0% to 20.4%. The height of the cavity and the slot thickness are adjusted among multiples of 0.2 mm or 0.3 mm because of fabrication limitations. The thinner cavity realizes a wider bandwidth. The reduction in the cavity height indirectly leads to a lower Q of the radiation slots. Sub-arrays with 0.8-mm and 1.0-mm cavity heights with 0.2-mm slot thickness are designed. For the impedance matching, mainly a, w_x, and slightly d_x, d_l, and w_{cp} are adjusted for each cavity height. The bandwidth is improved from 18.0% to 21.3% by reducing the cavity height from 1.20 mm to 0.80 mm as shown in Fig. 5 (Step 3). However, the 0.80-mm cavity height model generates grating lobes because the higher order modes do not attenuate sufficiently. The grating lobes degrade directivity bandwidth. Finally a 1.00-mm cavity height model was adopted as the best design model. The design reflection coefficient is shown in Fig. 8 (solid line) together with the conventional reflection coefficient (dashed line). The reflection bandwidth of VSWR < 1.5 is improved from 9.2% up to 20.4%. All the parameters of the designed model are listed in the Table 1.

4.2 Results with Simulations of the 16×16-Element Array

The 16×16-elment array is composed of the designed 2×2-element sub-array and the feeding waveguide and was analyzed by HFSS. The conductivity of copper is assumed to

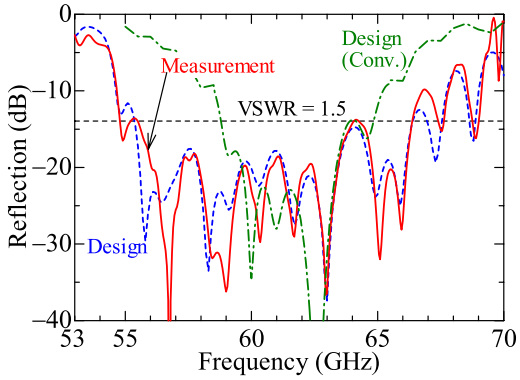

Fig. 9 Frequency characteristics of reflection.

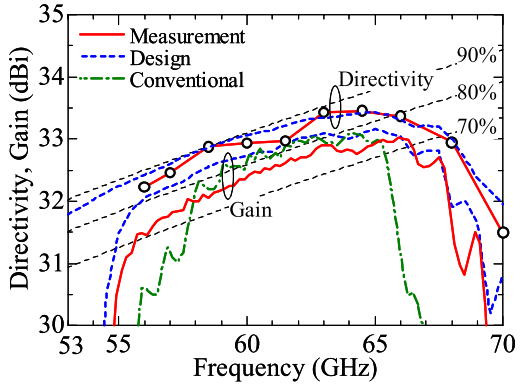

Fig. 10 Frequency characteristics of directivity and gain.

be 5.8×10^7 S/m. The frequency characteristics of reflection are shown in Fig. 9 (dashed line). The bandwidth of VSWR < 1.5 is improved to 18.5% (11.2 GHz, 55.2–66.4 GHz) from the 8.3% with the conventional sub-array (chained line). The frequency characteristics of the gain are shown in Fig. 10 (dashed line). At the design frequency, 32.9-dBi gain is obtained and the corresponding antenna efficiency is 82.3%, where aperture size is defined as a square of 67.2 mm (= 16 elements × 4.2 element spacing) with 0.27-dB conductor loss. The bandwidth of the gain > 31.5 dBi is im-

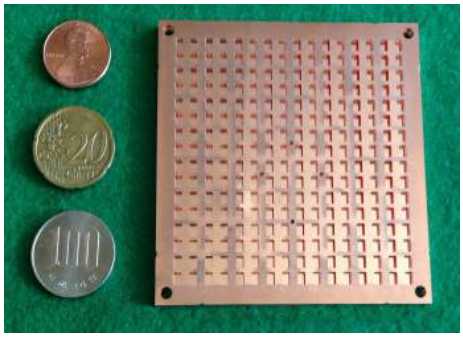

Fig. 11 Photo of the fabricated antenna.

proved up to 22.7% (14.1 GHz, 55.0–69.1 GHz) from 14.2% because of the reflection bandwidth improvement of the sub-array.

5. Experimental Results

5.1 Fabrication

The antenna was fabricated by diffusion bonding of thin copper plates. The fabrication method caused an over- or under-etching and misalignment among the bonded plates as a result of fabrication tolerances [12], [19], [20]. Considering the effect of both kinds of errors, we estimated a 20-μm equivalent over-etching amount in one side in all the antenna parameters. Therefore, the antenna was fabricated by compensating for an equivalent amount of over-etching. A photo of the fabricated antenna is shown in Fig. 11. The total thickness is 3.2 mm. Eight through holes are made in the four corners and around the feeding aperture for setting it in the jig for the measurements. The dimensions of each plate are 75 mm × 76 mm × 0.2 mm.

5.2 Reflection

The measured frequency characteristics of the reflection is shown in Fig. 9 (solid line) with the design frequency characteristics (dashed line). They agree well in terms of absolute values and resonance frequencies. This indicates that the equivalent over-etched amount is around 20 μm and that the design compensates for the fabrication errors in the reflection. The bandwidth of VSWR below 1.5 and 2.0 is 14.3%, 8.6 GHz (55.5–64.1 GHz) and 21.5%, 13.2 GHz (54.7–67.8 GHz), respectively. The maximum value of the reflection in the 60-GHz band is −13.8 dB at 64.2 GHz.

5.3 Gain and Efficiency

The measured frequency characteristics of gain and directivity are shown in Fig. 10. At the design frequency, 32.6-dBi gain, 33.0-dBi directivity, and 76.5% antenna efficiency is obtained. Further, a constant antenna efficiency is achieved over a broad bandwidth. The bandwidth for a gain of more than 31.5 dBi is improved greatly, to 19.2% (11.9-GHz bandwidth: 56.1–68.0 GHz) from the conventional design with 13.1% bandwidth. The maximum degradation of the directivity and the gain from the design values is 0.2 dBi and 0.4 dBi over the bandwidth, respectively.

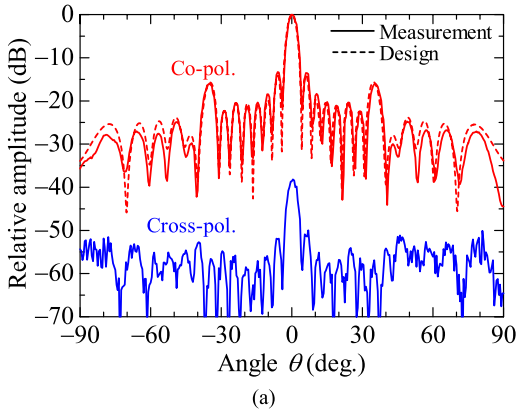

(a)

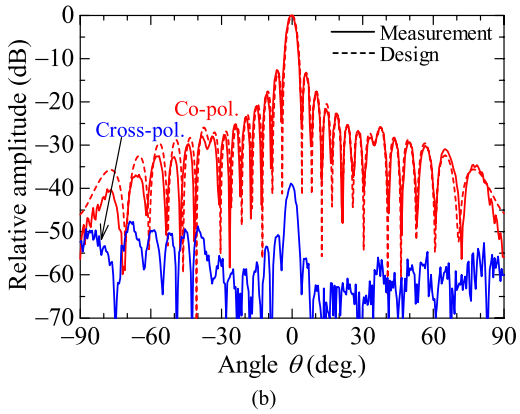

(b)

Fig. 12 Radiation patterns at 61.5 GHz. (a) E-plane. (b) H-plane.

5.4 Radiation Pattern

The measured radiation patterns in the E- and H-planes at the design frequency are shown in Fig. 12. The measured patterns agree well with the simulated ones. The first sidelobe level in the E-plane is −13.3 dB. There are −16.1-dB grating lobes at the $\theta = \pm 35.5^\circ$ directions in the E-plane because of the 2.0-dB and 37-degree excitation difference between the two edges of a slot in the width direction which is the same as the E-plane direction. The excitation difference occurred because of wider radiating slots and lower cavity heights than the ones in [12]. The wide slots cause a non-uniform electromagnetic field in the width direction. The low cavities propagate unwanted higher order modes and lead to non-uniform excitation on the slot apertures. Cross polarization levels at the boresight in the E-plane is −38.2 dB. The E-plane radiation patterns at 58.0, 61.5, and 65.0 GHz are shown in Fig. 13. The main beam direction is the boresight and unchanged over the bandwidth. The first sidelobe levels, the grating lobe levels, and the cross polarization levels are detailed in Table 2.

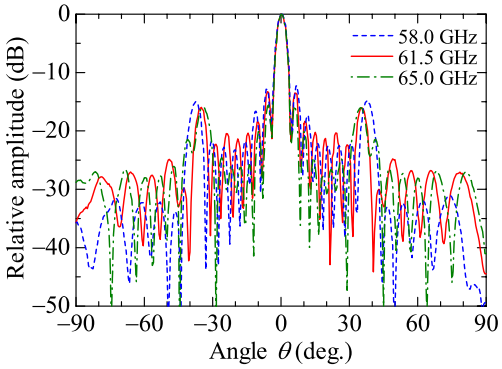

Fig. 13 Radiation patterns in the E-plane at 58.0, 61.5 and 65.0 GHz.

Table 2 First sidelobe levels and grating lobe levels in the E-plane.

Frequency (GHz)	First Sidelobe Level (dB)	Grating Lobe Level (dB)	Cross Polarization Level (dB)
58.0	−12.3	−14.8	−40.0
61.5	−13.3	−16.1	−38.2
65.0	−15.7	−16.0	−36.4

5.5 Aperture Field Distribution

The aperture field distributions reflect the uniformity of the diffusion bonding on the plates in the fabrication process. The measured aperture field distribution at the design frequency is shown in Fig. 14. Symmetrical distributions along the x- and y-axes are obtained. Hence, uniform bonding between the plates is realized across the plates. The amplitude ripples along the x-axis are caused by the excitation differences in the radiating slots and the truncation effect of the array arrangement. The excitation differences occur due to the wide radiating slots and the thin cavities as explained in Sect. 5.4. The truncation of the array arrangement affects the aperture distribution in the E-plane direction because the element pattern of the slot in the E-plane is non-directional and the effect of mutual coupling is large.

6. Conclusion

A 16 × 16-element waveguide slot array antenna in the 60-GHz band was designed and fabricated. The resulting broadband high gain antenna offers a 32.6 dBi gain, 21.5% reflection bandwidth of VSWR < 2, and 19.2% bandwidth of gain > 31.5 dBi by enhancing the reflection bandwidth of the sub-array. The 19.2% gain bandwidth (11.9 GHz: 56.1–68.0 GHz) covers the whole of the license-free 60-GHz band (57–66 GHz). The fabricated antenna is suitable for a high speed fixed wireless communication system. The wideband design method described here can be applied to other types of corporate-feed waveguide slot arrays to improve the reflection bandwidth of the sub-array and lead to improvements in the reflection and gain across the entire array.

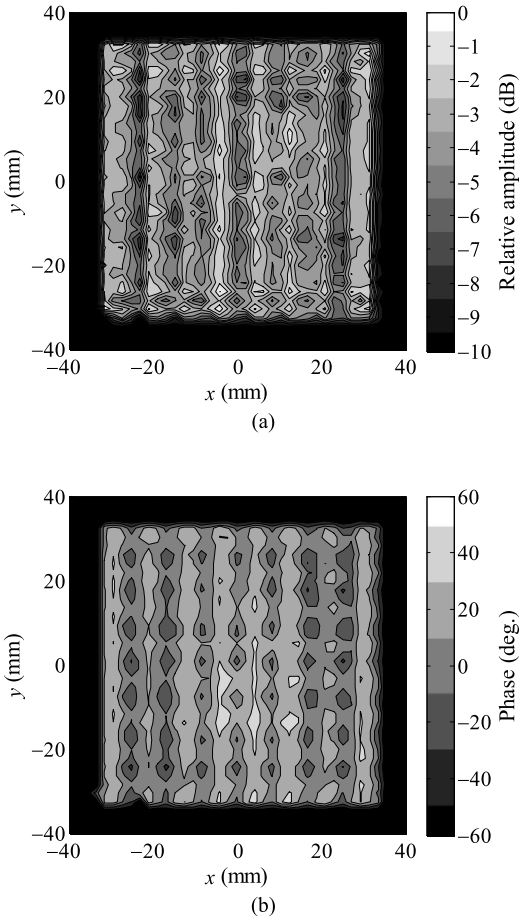

Fig. 14 Near-field distributions at 61.5 GHz. (a) Amplitude. (b) Phase.

References

[1] R. Fisher, "60 GHz WPAN standardization within IEEE 802.15.3c," Proc. Int. Signals, Syst. Electron Symp., pp.103–105, 2007.
[2] A. Hirata, R. Yamaguchi, T. Kosugi, H. Takahashi, K. Murata, T. Nagatsuma, N. Kukutsu, Y. Kado, N. Iai, S. Okabe, S. Kimura, H. Ikegawa, H. Nishikawa, T. Nakayama, and T. Inada, "10-Gbit/s wire-less link using InP HEMT MMICs for generating 120-GHz-band millimeter-wave signal," IEEE Trans. Microw. Theory Tech., vol.57, no.5, pp.1102–1109, May 2009.
[3] R.C. Johnson and H. Jasik, Antenna Engineering Handbook, ch. 9, McGraw-Hill, New York, 1984.
[4] N. Goto, "A planar waveguide slot antenna of single layer structure," IEICE Technical Report, AP88-39, 1988.
[5] Y. Kimura, Y. Miura, T. Shirosaki, T. Taniguchi, Y. Kazama, J. Hirokawamb, and M. Ando, "A low-cost and very compact wire-less terminal integrated on the back of a waveguide planar array for 26 GHz band fixed wireless access (FWA) systems," IEEE Trans. Antennas Propag., vol.53, no.8, pp.2456–2463, Aug. 2005.
[6] R.W. Haas, D. Brest, H. Mueggenburg, L. Lang, and D. Heimlich, "Fabrication and performance of MMW and SMMW platelet horn arrays," Int. J. Infrared Millim. Waves, vol.14, no.11, pp.2289–2294, 1993.
[7] M. Zhang, J. Hirokawa, and M. Ando, "Design of a partially-corporate feed double-layer slotted waveguide array antenna in 39 GHz band and fabrication by diffusion bonding of laminated thin metal plates," IEICE Trans. Commun., vol.E93-B, no.10, pp.2538–2544, Oct. 2010.

[8] M. Muller, I.P. Theron, and D.B. Davidson, "Improving the bandwidth of a slotted waveguide array by using a centre-feed configuration," Proc. IEEE Africon, vol.2, pp.1075–1080, 1996.
[9] J.C. Coetzee, J. Joubert, and W.L. Tan, "Frequency performance enhancement of resonant slotted waveguide arrays through the use of wideband radiators or subarraying," Microw. Opt. Technol. Lett., vol.22, no.1, pp.35–39, 1999.
[10] S.S. Oh, J.W. Lee, M.S. Song, and Y.S. Kim, "Two-layer slotted-waveguide antenna array with broad reflection/gain bandwidth at millimetre-wave frequencies," IEE Proc.-Microw. Antennas Propag., vol.51, no.5, pp.393–398, Oct. 2004.
[11] B. Lee, K. Jung, and S. Yang, "High-efficiency planar slot array antenna with a single waveguide-fed cavity-backed subarray," Microw. Opt. Technol. Lett., vol.43, no.3, pp.228–231, Nov. 2004.
[12] Y. Miura, J. Hirokawa, M. Ando, Y. Shibuya, and G. Yoshida, "Double-layer full-corporate-feed hollow-waveguide slot array antenna in the 60 GHz-band," IEEE Trans. Antennas Propag., vol.59, no.8, pp.2844–2851, Aug. 2011.
[13] J. Hirokawa, H. Arai, and N. Goto, "Cavity-backed wide slot antenna," Proc. Inst. Elect. Eng., pt. H, vol.136, no.1, pp.29–33, Feb. 1989.
[14] Y. Suzuki and T. Chiba, "Designing method of microstrip antenna considering the bandwidth," IEICE Trans., vol.E67, no.9, pp.488–493, Sept. 1984.
[15] A. Sabban, "A new broadband stacked two-layer microstrip antenna," Proc. IEEE AP-S Int. Symp., vol.21, pp.63–66, 23-26 May 1983.
[16] G. Kumar and K. Gupta, "Nonradiating edges and four edges gap-coupled multiple resonator broad-band microstrip antennas," IEEE Trans. Antennas Propag., vol.33, no.2, pp.173–178, Feb. 1985.
[17] T. Hirano, J. Hirokawa, and M. Ando, "Method of moments analysis of a waveguide crossed slot by using the eigenmode basis functions derived by the edge-based finite-element method," IEE Proc.-Microw. Antennas Propag., vol.147, no.5, pp.349–353, Oct. 2000.
[18] J.L. Volakis, A. Chatterjee, and L.C. Kempel, Finite Element method for Electromagnetics, IEEE Press, NY, 1998.
[19] T. Tomura, Y. Miura, M. Zhang, J. Hirokawa, and M. Ando, "A 45° linearly polarized hollow-waveguide corporate-feed slot array antenna in the 60-GHz band," IEEE Trans. Antennas Propag., vol.60, no.8, pp.3640–3646, Aug. 2012.
[20] Y. Miura, J. Hirokawa, M. Ando, K. Igarashi, and G. Yoshida, "A high-efficiency circularly-polarized aperture array antenna with a corporate-feed circuit in the 60 GHz band," IEICE Trans. Electron., vol.E94-C, no.10, pp.1618–1625, Oct. 2011.

Takashi Tomura was born in Sendai, Japan, on November 1, 1985. Tomura received the B.S. and M.S. degrees in Electrical and Electronic Engineering from the Tokyo Institute of Technology, Tokyo, Japan, in 2008 and 2011, respectively. He is currently working for the D.E. degree at the Tokyo Institute of Technology, Tokyo, Japan. At present, he is a Research Fellow of the Japan Society for the Promotion of Science (JSPS). His research interests include planar waveguide slot array antennas. He received the Best Student Award from Ericsson Japan in 2012.

Jiro Hirokawa was born in Tokyo, Japan, on May 8, 1965. He received his B.S., M.S., and D.E. degrees in Electrical and Electronic Engineering from the Tokyo Institute of Technology (Tokyo Tech), Tokyo, Japan in 1988, 1990, and 1994, respectively. He was a Research Associate from 1990 to 1996 and is currently an Associate Professor at Tokyo Tech. From 1994 to 1995, he was with the antenna group of Chalmers University of Technology, Gothenburg, Sweden, as a Postdoctoral Fellow. His research area has been in slotted waveguide array antennas and millimeter-wave antennas. He received an IEEE AP-S Tokyo Chapter Young Engineer Award in 1991; a Young Engineer Award from IEICE in 1996; a Tokyo Tech Award for Challenging Research in 2003; a Young Scientists' Prize from the Minister of Education, Cultures, Sports, Science and Technology in Japan in 2005; a Best Paper Award in 2007; and a Best Letter Award in 2009 from IEICE Communication Society and Asia Pacific Microwave Conference prize in 2011 and 2012. He is a Fellow of the IEEE.

Takuichi Hirano was born in Tokyo, Japan, on January 28, 1976. He received the B.S. degree in electrical and information engineering from the Nagoya Institute of Technology, Nagoya, Japan, in 1998, and the M.S. and D.E. degrees from the Tokyo Institute of Technology, Tokyo, Japan, in 2000 and 2008, respectively. He is currently an Assistant Professor with the Tokyo Institute of Technology. He has been involved with EM theory, numerical analysis of EM problems, and antenna engineering including slotted waveguide arrays. Dr. Hirano is a member of the IEEE, the Institute of Electronics, In-formation and Communication Engineers (IEICE), and the Institute of Electrical Engineers of Japan (IEEJ). He was the recipient of the Young Engineer Award of the IEICE, the IEEE Antennas and Propagation Society (AP-S) Japan Chapter Young Engineer Award in 2004, the IEEJ Excellent Presentation Award, the IEEE MTT-S Japan Young Engineer Award in 2011.

Makoto Ando was born in Hokkaido, Japan, on February 16, 1952. He received his B.S., M.S., and D.E. degrees in Electrical Engineering from the Tokyo Institute of Technology, Tokyo, Japan in 1974, 1976, and 1979, respectively. From 1979 to 1983, he worked at the Yokosuka Electrical Communication Laboratory, NTT, and was engaged in the development of antennas for satellite communication. He was a Research Associate at the Tokyo Institute of Technology from 1983 to 1985 and is currently a Professor. His main interests have been high-frequency diffraction theory, such as Physical Optics and Geometrical Theory of Diffraction. His research also covers the design of reflector antennas and waveguide planar arrays for DBS and VSAT. Latest interests include the design of high-gain millimeter-wave antennas. He received the Young Engineers Award in 1981, the Achievement Award in 1993, and the Paper Awards in 2009, all from IEICE Japan. He also received the 5th Telecom Systems Award in 1990, the 8th Inoue Prize for Science in 1992, the Meritorious Award of the Minister of Internal Affairs and Communications and the Chairman of the Board of ARIB in 2004, and the Award in Information Promotion Month 2006, the Minister of Internal Affairs and Communications. He served as the guest editor-in-chief of more than six special issues in IEICE, Radio Science, and IEEE AP. He was the general chair of the 2004 URSI EMT symposium in Pisa and the ISAP 2007 in Niigata. He served as the chair of the Technical committee of Electromagnetic theory (2004–2005) and Antennas and Propagation (2005–2007) in IEICE. He served as the member of the Administrative Committee of IEEE Antennas and Propagation Society from 2004 to 2006 and also as the member of the Scientific Council for Antenna Centre of Excellence (ACE) in EU's 6th framework program since 2004. He served as the Chair of Commission B of URSI from 2002 to 2005. He was the 2007 President of Electronics Society IEICE and the 2009 President of IEEE Antennas and Propagation Society. He is currently serving as the Program Officer for the Engineering Science Group in the Research Center for Science Systems, JSPS. He is a Fellow of IEEE and IEICE.